Journal of Asian Earth Sciences 259 (2024) 105927

Contents lists available at ScienceDirect

Journal of Asian Earth Sciences

journal homepage: www.elsevier.com/locate/jseaes

The influence of asphaltene matrix on the thermal evolution of polycyclic aromatic hydrocarbons: Experimental evidence and geochemical implications

Peng Fang [a,b,*], Zhibin Hong [a], Jia Wu [a,b,**], Yuan Wang [c], Keyu Liu [d], Minghui Zhou [e]

[a] National Key Laboratory of Petroleum Resources and Engineering, China University of Petroleum (Beijing), Beijing 102249, China
[b] State Key Laboratory of Organic Geochemistry, Guangzhou Institute of Geochemistry, Chinese Academy of Sciences, Guangzhou 510640, China
[c] Wuxi Research Institute of Petroleum Geology, Petroleum Exploration and Production Research Institute, SINOPEC, Wuxi, Jiangsu 214216, China
[d] School of Geosciences, China University of Petroleum (East China), Qingdao, Shandong 266580, China
[e] State Key Laboratory of Enhanced Oil and Gas Recovery, Research Institute of Petroleum Exploration and Development, PetroChina, Beijing 100083, China

ARTICLE INFO

Keywords:
Asphaltenes
Adsorbed/Occluded hydrocarbons
Polycyclic aromatic hydrocarbons
Thermal evolution
Maturity

ABSTRACT

The thermal evolution of components trapped in matrix of asphaltenes is supposed to be retarded, as compared to the free ones. Studying the geochemical evolution of trapped polycyclic aromatic hydrocarbons (PAHs) may provide insight for the characterization of high-maturity organic matter. The discrepancies in the thermal evolution between free and trapped (asphaltene-adsorbed/occluded) PAHs (phenanthrene, chrysene, pyrene, and their methylated isomers) were studied by thermal maturation (gold tubes, 300 ~ 400 °C) experiments on a low-maturity solid bitumen from the Sichuan Basin, southwestern China. The results show that the thermal evolution of asphaltene-adsorbed PAHs is retarded compared to that of free ones. This is attributed to slight differences in reaction kinetics due to steric hindrance by the asphaltene structure. The asphaltene matrix appears to act as a reaction inhibitor leading to a retardation of the thermal evolution of the methylphenanthrene index (MPI) in asphaltene-adsorbed hydrocarbons. This could provide a possibility for maturity assessment of high-maturity organic matter. The thermal evolution of asphaltene-occluded PAHs in the experiments resulted in thermodynamically controlled isomer distributions of occluded methylphenanthrenes and methylchrysenes. However, the occluded methylpyrene isomers were hardly affected by thermal stress. They probably retained their original distributions and may serve as source indicators.

1. Introduction

The maturity assessment of sedimentary organic matter (OM) is essential in basin thermal history analysis and petroleum exploration (Robert, 1988). Vitrinite reflectance (R_o) is recognized as a reliable indicator of OM maturity, but it is not conditioned for liquid petroleum (Tissot et al., 1987). The isomerization parameters of biomarkers (such as hopanes and steranes) are also applied to assess the maturity of both source rocks and petroleum (Seifert and Moldowan, 1980; Huang et al., 1990). However, the isomerization parameters are not sensitive to maturity after the "oil-generating window" and thus lose the indicative significance (Huang et al., 1990; Peters et al., 2004). Furthermore, mineral catalysis and secondary alterations, such as biodegradation or migration, can easily change the distributions of biomarkers (Spiro, 1984; Tannenbaum et al., 1986; Liu et al., 2022).

In contrast, polycyclic aromatic hydrocarbons (PAHs) stably existing in petroleum are suitable for evaluating OM with medium to high maturity (Kvalheim et al., 1987; Radke, 1988; Kruge, 2000). PAHs are generally considered to be secondary products during the thermal evolution of sedimentary OM, so their compositions are mainly controlled by the extent of thermal evolution (Tissot and Welte, 1984). Various maturity parameters based on the relative compositions of bicyclic to pentacyclic aromatics have been proposed by different authors (Garrigues et al., 1988; Radke et al., 1994; Rospondek et al., 2009; Li et al., 2012; Fang et al., 2015; Li et al., 2016; Zhu et al., 2019; Zhu et al., 2022). For instance, typical tricyclic aromatic hydrocarbon parameters such as MPI (see equation (1) and (2)) and MDR (see equation (3)) have a positive correlation with vitrinite reflectance (Radke, 1982; Radke et al.,

* Corresponding author at: National Key Laboratory of Petroleum Resources and Engineering, China University of Petroleum (Beijing), Beijing 102249, China.
** Corresponding author at: National Key Laboratory of Petroleum Resources and Engineering, China University of Petroleum (Beijing), Beijing 102249, China.
E-mail addresses: 2020310023@student.cup.edu.cn (P. Fang), jia.wu@cup.edu.cn (J. Wu).

https://doi.org/10.1016/j.jseaes.2023.105927
Received 12 July 2023; Received in revised form 15 September 2023; Accepted 11 November 2023
Available online 13 November 2023
1367-9120/© 2023 Elsevier Ltd. All rights reserved.

1986; Radke, 1988). However, the positive correlation will reverse as OM maturity advanced, which limits the application of these parameters (Radke, 1982; Wu et al., 2019).

$$MPI_1 = \frac{1.5*(2-MP+3-MP)}{P+1-MP+9-MP} \quad (1)$$

$$MPI_2 = \frac{3*(2-MP)}{P+1-MP+9-MP} \quad (2)$$

$$\mathrm{MDR} = \frac{\text{4-MDBT}}{\text{1-MDBT}} \quad (3)$$

In order to overcome the shortcomings of molecular markers in maturity assessment of OM, asphaltenes and asphaltene-associated components have recently been investigated (Orea et al., 2021; Sadeghtabaghi et al., 2021; de Lima et al., 2022; Sadeghtabaghi et al., 2022). Asphaltene-associated components commonly refer to the small molecules trapped (adsorbed or occluded) by asphaltene structure through noncovalent bonding (Zhao et al., 2010; Zhao et al., 2012; Chacón-Patiño et al., 2016; Snowdon et al., 2016; Cheng et al., 2017; Evdokimov and Losev, 2020). It has been reported in many literatures that there are two kinds of asphaltene molecular structure models, island and archipelago (Mullins, 2010; Mullins, 2011; Mullins et al., 2012; Chacón-Patiño et al., 2017b; Chacón-Patiño et al., 2017a; Chacón-Patiño et al., 2018). Two kinds of asphaltene molecules can form complex supramolecular structures (also known as molecular aggregates) under conditions of intermolecular forces (Gray et al., 2011). GPC (Gel Permeation Chromatography) tests show that these complex aggregation structures are dispersed under solvent dilution (González et al., 2020; Castillo et al., 2023), which is similar to the connotation of the Yen-Mullins model (Mullins, 2010; Mullins, 2011; Mullins et al., 2012). Therefore, solvent dilution can release small molecules trapped by asphaltene aggregates.

In addition to trapped saturated biomarkers observed in the reservoir, there may be a series of PAHs trapped in the asphaltene matrix (Derakhshesh et al., 2013; Wu et al., 2020; de Lima et al., 2022; Fang et al., 2022a). Due to the restriction of macromolecular structure, trapped (adsorbed or occluded) PAHs potentially influenced by thermal stress theoretically evolve slower than free PAHs (Cheng et al., 2016). Therefore, it is a potential approach to assess high-maturity organic matter by revealing the geochemical evolution of asphaltene-trapped PAHs.

To verify this hypothesis, the evolution discrepancies of specific PAHs under different occurrence states (free state and asphaltene-adsorbed/occluded state) in asphaltene matrix were investigated. Low-maturity natural solid bitumen was selected as the sample, from which the asphaltene was extracted for experiments. Closed-system pyrolysis experiments and dispersive solid-phase extraction were conducted to obtain aromatics trapped by the asphaltene matrix with different degrees of thermal evolution (Fang et al., 2022b). Through the systematic comparison of specific PAH products and the analysis of the theoretical thermodynamic data calculated by the Gaussian 09 program, the thermal evolution characteristics of aromatics in different occurrence states and its significance were elucidated.

2. Materials and methods

2.1 Sample

A solid bitumen sample was collected from the lower Cambrian Changjianggou formation outcrop in the Kuangshanliang region, northwestern Sichuan Basin, southwestern China. The chemical composition has been analyzed by previous study (Liang et al., 2020). This solid bitumen has a low maturity with equivalent vitrinite reflectance values ranging from 0.5 % to 0.8 %.

2.2 Chemicals

Analytical-grade petroleum ether (30 ~ 60 °C boiling range) and dichloromethane (DCM) were purchased from Tianjin Jindong Tianzheng Fine Chemical Reagent Factory in China and re-distilled immediately before use.

Chromatography grade silica gel procured from Aladdin Reagent (Shanghai) Co., Ltd., and alumina procured from Alfa Aesar (China) Chemicals Co., Ltd. were used to prepare the columns for liquid/solid chromatographic separation of the compound groups.

2.3 Solvent extraction and asphaltene preparation

Approximately 1.5 g of the solid bitumen was ground to around 100 mesh with an agate mortar and the soluble OM was extracted with dichloromethane (DCM) in a Soxhlet apparatus (Wu et al., 2020). After evaporating the DCM extract to dryness (approximately 0.5 g), 50 mL of petroleum ether were added and the mixture thoroughly ultrasonicated. The insoluble asphaltene fraction was then separated from the dissolved maltenes by filtration.

The maltene solution was evaporated to dryness, weighed, re-dissolved in 2 mL of petroleum ether and placed on a silica gel/alumina (3:2) column. The saturate fraction was eluted from the column by petroleum ether (Zhu et al., 2022) and the aromatic fraction was eluted in a second step with a DCM/petroleum ether (2:1, v/v) mixture. An aliquot of this aromatic fraction was termed the “free aromatics”.

The asphaltene fraction was re-dissolved in a small amount of DCM, precipitated again by adding an excess of petroleum ether and then purified by centrifugation (3500 rpm for 20 min) (Liao et al., 2006a; Liao et al., 2006b; Wu et al., 2020). The supernatant petroleum ether extract, containing the “asphaltene-adsorbed components”, was again evaporated to dryness and the aromatic compounds were (“asphaltene-adsorbed aromatics”) isolated by column chromatography.

2.4 Thermal maturation experiments

Thermal maturation experiments of the purified asphaltenes were conducted in an ST-120-II gold tube reactor (Wu et al., 2020; Fang et al., 2022a). The wall thickness, the inner diameter, and the length of the gold tubes were 0.25, 5.5, and 60 mm, respectively. The tubes were filled with approximately 30 mg of asphaltenes and 100 mg of deionized water and then sealed by argon arc welding to prevent the access of atmospheric oxygen. They were placed into the autoclave vessel and pressurized to 30 MPa (296.08 atm). The autoclave vessel was then heated to the target temperatures of 300 °C (T-300), 350 °C (T-350), and 400 °C (T-400) within one hour and kept at this temperature for 24 h. The calculated vitrinite reflectance values using the Easy%R_o model (Sweeney and Burnham, 1990) were 0.64 %, 0.92 % and 1.49 % for the 300 °C, 350 °C and 400 °C experiments, respectively. The gold tubes were recovered after the autoclave vessel had cooled to room temperature.

2.5 Isolation of the asphaltene-trapped components

The isolation procedure for the products of the thermal maturation experiments is shown in Fig. 1. The gold tubes were cut open, immersed in petroleum ether (30 ~ 50 mL) and ultrasonicated for 20 ~ 30 min at room temperature. The extraction procedure was repeated three times with fresh petroleum ether. The combined petroleum ether extracts, termed “free components”, were isolated by column chromatography to obtain “free aromatics”. The asphaltenes in solid residue were extract with DCM and purified by centrifugation (3500 rpm for 20 min). At the same time, the “asphaltene-adsorbed components” were acquired and then isolated by column chromatography to obtain “asphaltene-adsorbed aromatics”.

The purified asphaltenes were subjected to dispersive solid-phase

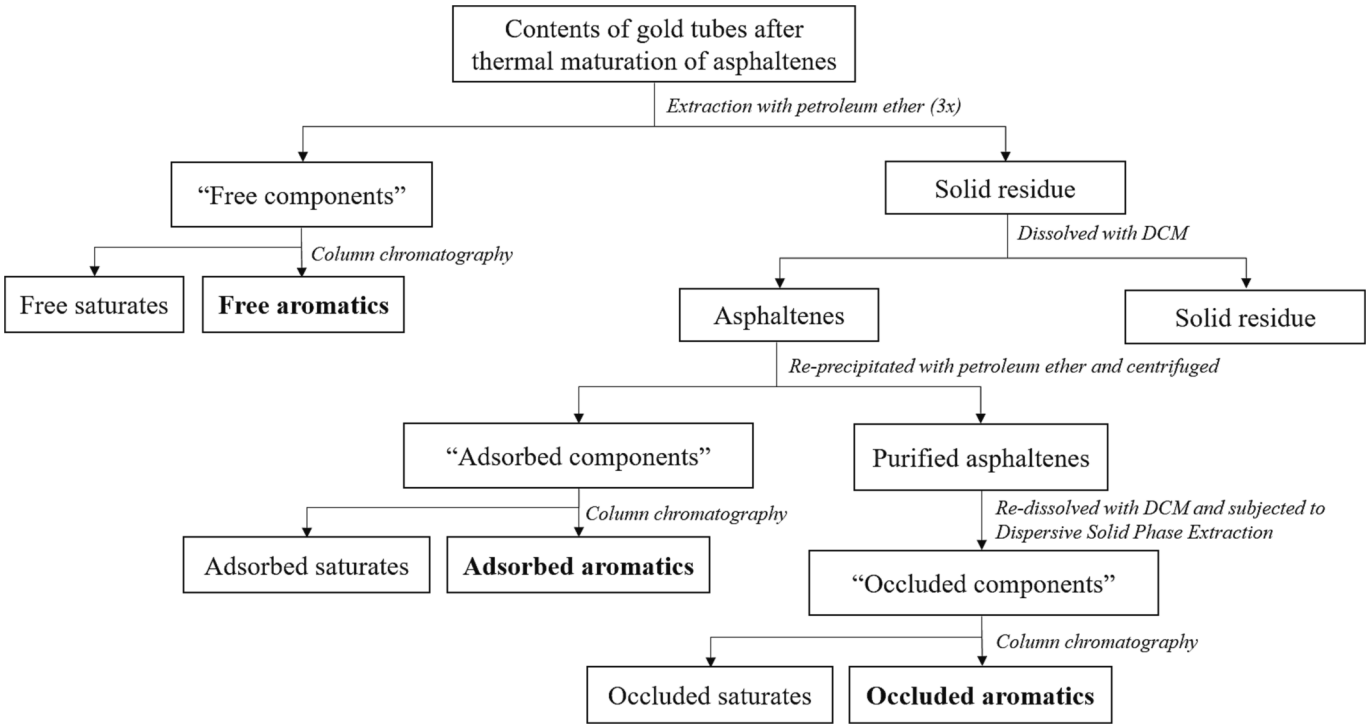

Fig. 1. Isolation procedure for aromatic compounds from original extracts ("free aromatics"), asphaltenes ("adsorbed aromatics") and the re-precipitated asphaltenes ("occluded aromatics").

extraction using silica gel and DCM (Fang et al., 2022a; Fang et al., 2022b) to access the "asphaltene-occluded components". The purified asphaltenes were dissolved by ultrasonication in an excess of DCM to obtain a concentration of approximately 0.1 mg/mL (Castillo et al., 2023). Approximately 5 g of silica gel (100 ~ 200 mesh) was then gradually added to the solution while stirring with a magnetic stirrer for 0.5 h. The silica gel particles were allowed to settle, filtrated and washed at least three times with DCM. All filtrates were combined in a flask and concentrated to 2 ~ 3 mL by rotatory evaporation. The aromatics in the concentrate, defined as "asphaltene-occluded aromatics", were isolated by column chromatography as described above.

2.6 GC–MS analysis

GC–MS analyses of the aromatics were conducted using an Agilent 5975i mass spectrometer, coupled with an HP 6890 GC equipped with an HP-5MS fused silica capillary column (60 m length × 0.25 mm inner diameter × 0.25 μm film thickness). The GC conditions were as follows: (1) helium was used as the carrier gas (1 mL/min); (2) the split injector temperature was set to 300 °C; (3) 80 °C initial temperature held for 1 min, then raised to 310 °C at 3 °C/min and held isothermally for 18 min. The MS conditions were electron impact (EI) mode, ionization energy of 70 eV and a scan range of 50 ~ 450 Da. The total ion current (TIC) data and selected ion monitoring (SIM) data were collected at the same time. Compounds of interest were identified by searching the NIST MS Search 2.0 data library and comparison with literature data (Kruge, 2000; Li et al., 2012; Fang et al., 2015).

2.7 Quantum chemical calculations

To estimate the thermal stability of PAHs, quantum chemical calculations were performed for some methylated aromatics using the density functional theory (DFT) of the Gaussian 09 software (Yang et al., 2019; Zhu et al., 2022).

The geometries were optimized for the gas phase at 25 °C and 1 atm using the M062X/6-311G* level of theory (Zhao and Truhlar, 2008). Based on the geometric optimization, the single-point calculations were also carried out using the def2-TZVP basis set (Weigend and Ahlrichs, 2005). The Gibbs free energy (ΔG) was estimated by adding the thermal correction to the free energy of geometric structure optimization to the single point energy. In addition, geometric optimizations and single-point calculations were also carried out for the experimental temperature–pressure conditions. The solvent effect of water was taken into account by selecting the SRCF keyword with the SMD model option (SMD, solvent = water) in Gaussian.

3. Results

3.1 Composition of the aromatic fractions

In the thermal maturation experiments, the amounts of coke increased, while the proportion of soluble OM decreased significantly with reaction temperature. Table 1 lists the amounts of asphaltenes, maltenes and asphaltene-trapped (adsorbed/occluded) aromatics.

The distributions of PAHs (phenanthrene, pyrene, and chrysene) and their methylated homologs produced at different reaction temperatures are shown in Figs. 2-4. Phenanthrene (P) and the methylated isomers 3-MP, 2-MP, 9-MP, and 1-MP were identified in the phenanthrene series; Benzo[a]anthracene (BaA), Chrysene (Chy) and the methylated chrysene isomers 3-MChy, 2-MChy, 6-MChy, and 1-MChy were identified in the chrysene series; Pyrene (Pyr) and the methylated isomers 1-MPyr, 2-MPyr, and 4-MPyr were identified in the pyrene series (Figs. 2-4). The relative compositions of PAHs in the adsorbed aromatics in the raw sample were similar to those in the occluded aromatics but different from those in the free ones. For the products after thermal maturation, the relative abundances of free and adsorbed methylated PAHs gradually increased with temperature, while those of the occluded PAHs were stable.

The relative proportions of methylated isomers in the free and adsorbed aromatics varied significantly with thermal stress (Table 2). However, the relative proportions of methylated isomers in occluded aromatics were generally stable.

Table 1
Amounts of products of thermal maturation (gold tubes) of asphaltenes isolated from Changjianggou solid bitumen.

Sample Number	Raw asphaltenes (mg)	Free maltenes		Asphaltenes		Adsorbed aromatics		Occluded aromatics	
		Masses (mg)	Yields (wt.%)	Masses (mg)	Yields (wt.%)	Masses (mg)	Yields (wt.%)	Masses (mg)	Yields (wt.%)
T-300	30.5	0.4	1.3	20.3	66.6	0.2	0.7	0.3	1.0
T-350	30.6	1.4	4.6	15.5	50.7	< 0.1	< 0.3	< 0.1	< 0.3
T-400	30.3	2.9	9.6	3.0	9.9	< 0.1	< 0.3	< 0.1	< 0.3

Note: The detection limit and the precision are 0.1 mg. Samples numbers indicate the reaction temperatures. Adsorbed aromatics were isolated from asphaltenes by dissolution with DCM, re-precipitation with petroleum ether followed by column chromatography. Occluded aromatics were isolated by dispersive solid phase extraction of the purified asphaltenes and column chromatography of the maltenes in the supernatant.

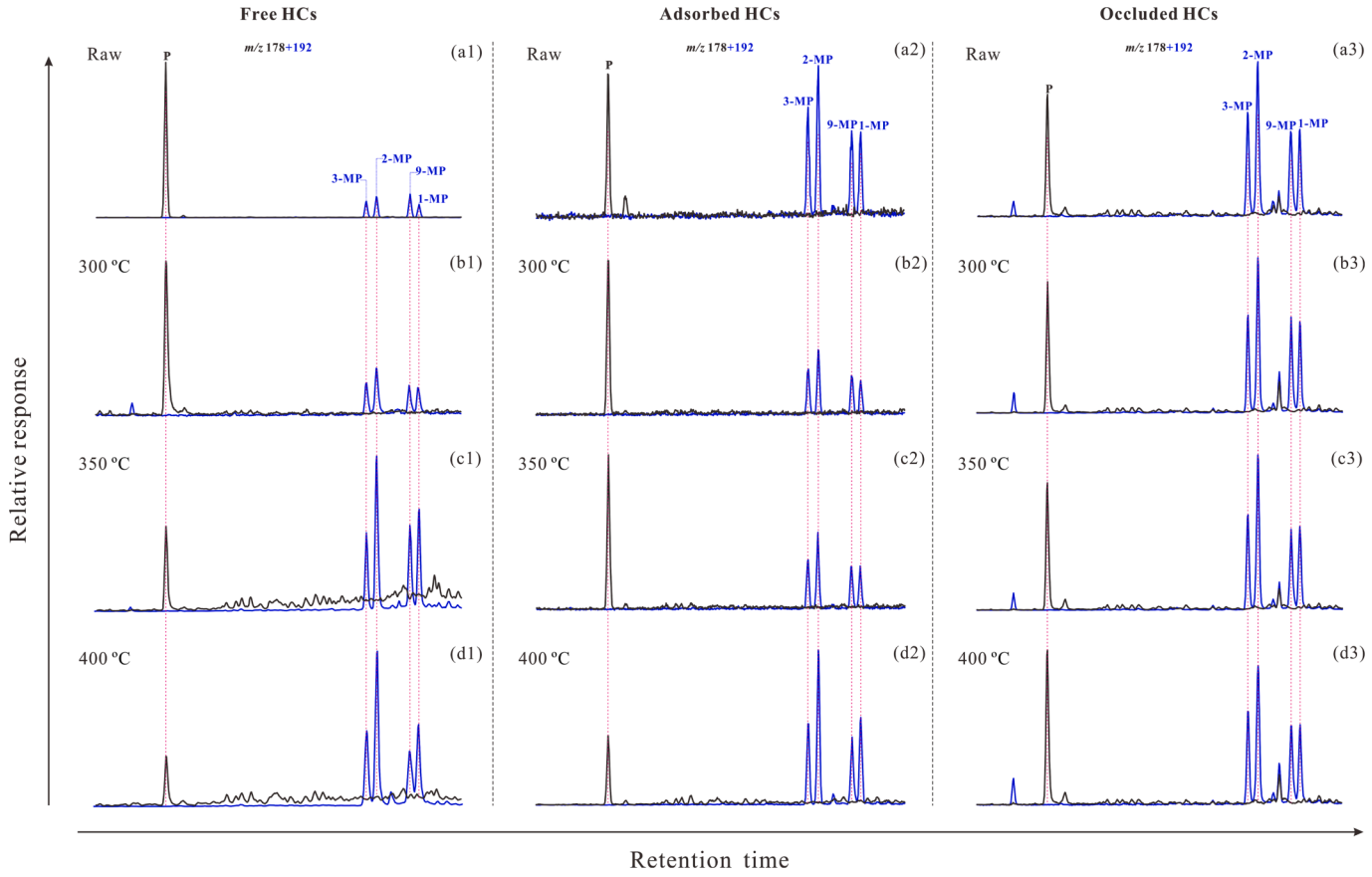

Fig. 2. Selected ion monitoring chromatograms of phenanthrene and methylphenanthrenes in the free, adsorbed and occluded aromatic fractions (P, Phenanthrene; 3-MP, 3-methyl phenanthrene; 2-MP, 2-methyl phenanthrene; 9-MP, 9-methyl phenanthrene; 1-MP, 1-methyl phenanthrene).

The relative proportions of the occluded methylphenanthrenes decreased in the order 2-MP, 3-MP, 9-MP, and 1-MP. The relative proportions of the occluded methylchrysenes decreased in the order 3-MChy, 2-MChy, 6-MChy, and 1-MChy for the original sample, while the relative proportions of 1-MChy were higher than those of 6-MChy after heat treatment. The relative proportions of the occluded methylpyrenes decreased in the order 4-MPyr, 2-MPyr and 1-MPyr.

3.2 PAH-based maturity parameters

In the free and adsorbed phenanthrene series, the parameters MPI_1, MPI_2, MPRn (n = 2,3,9,1) and the ∑MP/P increased with the calculated R_o, while the MPDF was relatively stable. The MPR fluctuated slightly with thermal evolution (Table 3). In the free and adsorbed chrysene series, the parameters 1-/6-MChy, MCI*, and ∑MChy/Chy increased with maturity, while the 2-/1-MChy ratio did not vary much with thermal evolution (Table 4). In the free and adsorbed pyrene series, $MPyI_1$ and ∑MPyr/Pyr increased with maturity, while the other parameters showed no discernible correlation with thermal evolution (Table 5). All the above parameters were relatively stable for the occluded aromatics, except for the 1-/6-MChy ratio, which increased with thermal maturation.

3.3 Thermodynamic properties

The thermodynamic data of methylated isomers obtained by quantum chemical calculations are listed in Table 6. The Gibbs free energy (ΔG) values of the methylphenanthrene isomers increase in the order 2-MP, 3-MP, 9-MP, and 1-MP. The ΔG values of the methylchrysene isomers increase in the order 3-MChy, 2-MChy, 6-MChy, and 1-MChy at 25 °C and 1 atm, while the ΔG of 6-MChy is higher than that of 1-MChy under experimental temperature–pressure conditions. The ΔG values of the methylpyrene isomers increase in the order 2-MPyr, 4-MPyr, and 1-MPyr.

Under identical pressure and temperature conditions, the Gibbs free energy can be used to estimate the relative thermodynamic stability of

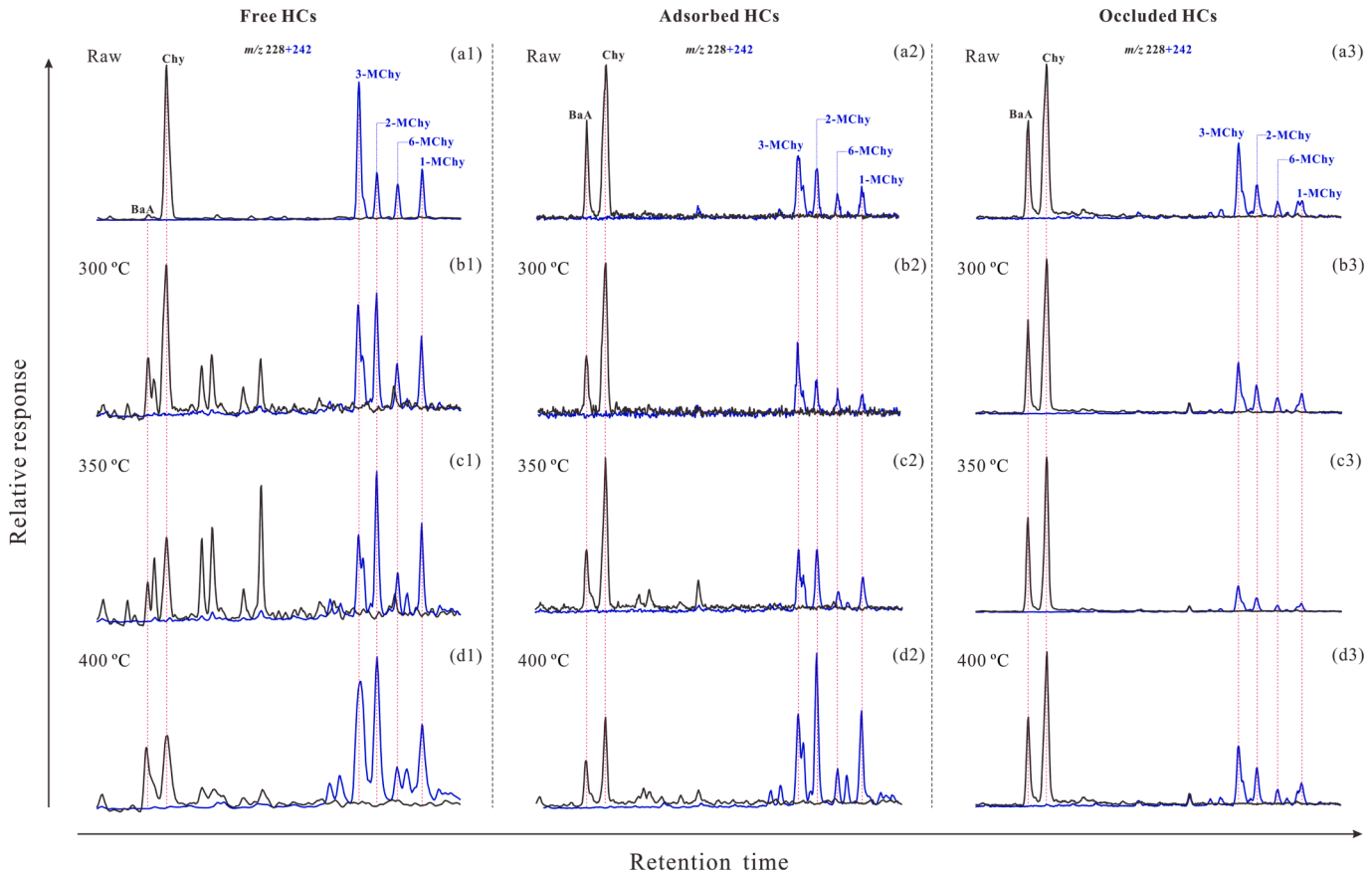

Fig. 3. Selected ion monitoring chromatograms of chrysene and methylchrysenes in the free, adsorbed and occluded aromatic fractions (BaA, Benzo[a]anthracene; Chy, Chrysene; 3-MChy, 3-methyl chrysene; 2-MChy, 2-methyl chrysene; 6-MChy, 6-methyl chrysene; 1-MChy, 1-methyl chrysene).

substances. In general, the higher the Gibbs free energy, the less stable the molecule. The thermal stability order of some PAH isomers has been estimated by previous workers using this principle (Zhu et al., 2022; Wang et al., 2023). The relative thermal stability values series of the compounds studied here are listed in Table 6 in the order of increasing ΔG. The order is consistent with the general view that the β isomers are more stable than the α isomers.

4 Discussions

4.1 Maturity parameters from PAHs in different aromatic fractions

4.1.1 Valid maturity parameters

Studies on the geological evolution of Type III kerogen showed an increase in the methylphenanthrene index (MPI) with maturity up to a vitrinite reflectance value R_o of 1.35 %, whereas the MPI correlated negatively with maturity at R_o values higher than 1.40 % (Radke, 1982; Radke et al., 1984; Radke, 1988). In this study, the MPI of the free and adsorbed aromatics were similar in the low maturity stage (Easy%R_o < 0.7). At calculated (Easy%R_o) vitrinite reflectance values below 1.5 %, the MPI_1 and MPI_2 of the free and adsorbed aromatics were positively correlated with thermal evolution without an inflection point or a downward trend (Fig. 5a & 5b). This is consistent with the results of thermal maturation experiments (Lu et al., 1996; Chen et al., 2023). At higher maturity levels, the values of the MPI and the maturity parameters based on tetracyclic aromatic compounds (MCI* and $MPyI_1$) were overall lower for the adsorbed aromatics than for the free aromatics (Fig. 5c & d). This indicates a retardation of the thermal evolution of adsorbed aromatics compared to the free aromatics.

Love et al. (1996) used pyridine to extract components "clathrated" within the macromolecular structure of vitrinite after the soluble OM (free components) had been extracted with DCM. The MPI values of the clathrated aromatics across the rank range investigated were lower than those of free aromatics. This was attributed to the restriction in the thermal evolution of small molecules by the reticular structure of coal macromolecules (Love et al., 1996). The chemical environment of the asphaltene-adsorbed aromatics in our study is considered similar to that of the clathrated components in vitrinite. Therefore, the observed retardation in the evolution of the maturity parameters of the adsorbed aromatics as compared to the free aromatics is also likely to result from a restriction by the structure of the asphaltene macromolecules.

4.1.2 Invalid maturity parameters

MPR is the ratio of the abundance of β isomers 2-MP to α isomers 1-MP, and MPDF represents the proportion of β isomers (2-MP and 3-MP) in the four methylphenanthrene isomers (Kvalheim et al., 1987; Radke, 1988). The slightly less stable α-isomers can be converted into the more stable β-isomers by methyl rearrangement under thermal stress. Therefore, MPR and MPDF have been proposed as indicators for the thermal maturity of sedimentary organic matter (Kvalheim et al., 1987; Radke, 1988; Nomoto et al., 2001). Based on this concept of the relative stability of isomers, other maturity parameters such as 2-/1-MChy, $MPyI_2$, and 2-/1-MPyr have been proposed, and it was shown in some case studies that these parameters did have a positive correlation with maturity (Garrigues et al., 1988; Kruge, 2000; Li et al., 2012; Fang et al., 2015).

However, for the free and adsorbed aromatics of the solid bitumen subjected to thermal maturation in this study, the above parameters did not show a significant correlation with the calculated vitrinite reflectance value R_o (Fig. 6a-f). The MP/P ratio (MPR1, MPR2, MPR3, MPR9), ∑MP/P, ∑MChy/Chy and ∑MPyr/Pyr of free and adsorbed aromatics gradually increased with R_o (Figs. 7 & 8), indicating a relative increase

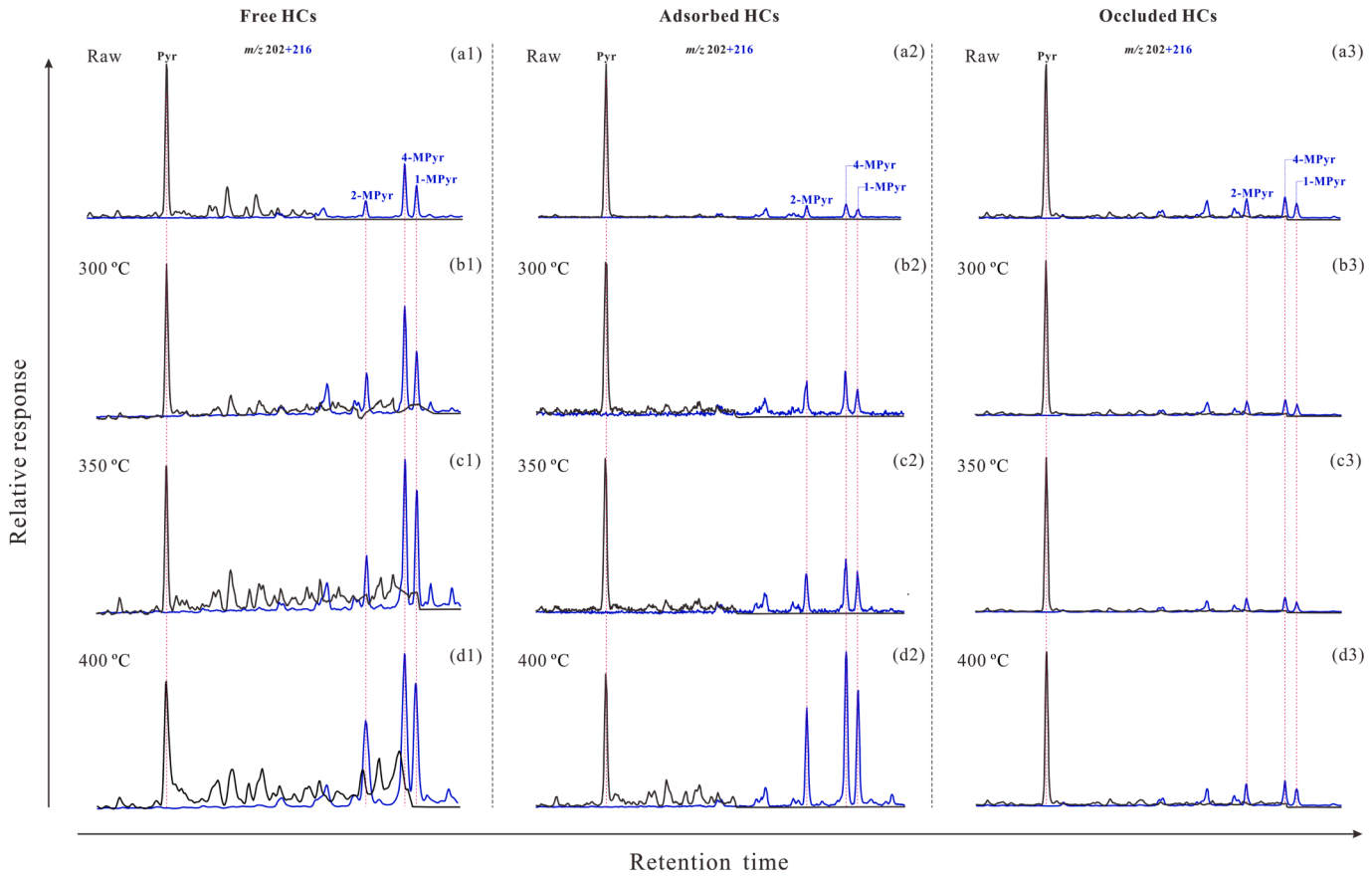

Fig. 4. Selected ion monitoring chromatograms of pyrene and methylpyrenes in the free, adsorbed and occluded aromatic fractions (Pyr, Pyrene; 2-MPyr, 2-methylpyrene; 4-MPyr, 4-methylpyrene; 1-MPyr, 1-methylpyrene).

Table 2
Relative proportions of methylphenanthrene, methylchrysene and methylpyrene isomers in the "free", "adsorbed" and "occluded" aromatic fractions of the Changjianggou solid bitumen after thermal (gold tube) maturation.

Fraction	Temperature (°C)	Methylphenanthrenes				Methylchrysenes				Methylpyrenes		
		3-MP	2-MP	9-MP	1-MP	3-MChy	2-MChy	6-MChy	1-MChy	2-MPyr	4-MPyr	1-MPyr
Free aromatics	Raw	0.22	0.29	0.31	0.18	0.52	0.17	0.13	0.18	0.18	0.50	0.32
	300°C	0.23	0.37	0.20	0.20	0.32	0.33	0.15	0.20	0.19	0.51	0.30
	350°C	0.18	0.37	0.21	0.24	0.31	0.35	0.12	0.22	0.17	0.48	0.35
	400°C	0.22	0.38	0.18	0.22	0.38	0.36	0.07	0.19	0.26	0.43	0.31
Adsorbed aromatics	Raw	0.23	0.30	0.31	0.16	0.42	0.29	0.12	0.17	0.18	0.50	0.32
	300°C	0.27	0.34	0.21	0.18	0.48	0.22	0.15	0.15	0.33	0.42	0.25
	350°C	0.23	0.36	0.21	0.20	0.32	0.35	0.12	0.21	0.32	0.40	0.28
	400°C	0.20	0.38	0.19	0.23	0.27	0.38	0.10	0.25	0.26	0.43	0.31
Occluded aromatics	Raw	0.23	0.37	0.21	0.19	0.52	0.23	0.13	0.12	0.35	0.38	0.27
	300°C	0.23	0.37	0.21	0.19	0.52	0.23	0.12	0.13	0.33	0.39	0.28
	350°C	0.22	0.37	0.21	0.20	0.53	0.24	0.10	0.13	0.36	0.38	0.26
	400°C	0.22	0.36	0.22	0.20	0.50	0.26	0.10	0.14	0.35	0.38	0.27

Note: The relative proportions of the isomers were calculated based on the peak areas in the selected ion monitoring chromatograms (Methylphenanthrenes, m/z = 192; Methylchrysenes, m/z = 242; Methylpyrenes, m/z = 216).

of methyl-substituted polyaromatic compounds during thermal maturation. It was found that the absolute contents of different methylphenanthrene isomers in coal samples increase with R_o in the early-middle stages of thermal evolution (Radke et al., 1990). A similar phenomenon was observed for methylpyrenes and methylfluoranthenes (Lu et al., 1996). Hence, parameters such as MPR and MPDF are unrelated to thermal maturity, probably due to the formation of a large quantity of methylated polyaromatics, especially in the early-middle stages of thermal maturation. The absence of a correlation between the proportion of newly generated aromatic methyl substitutes and their thermal stability is the most likely reason for the invalidity of the corresponding maturity parameters.

None of the molecular parameters determined for the asphaltene-occluded aromatics showed a correlation with maturity (Figs. 5-8). Occluded aromatics are small molecules isolated from the interior of asphaltene aggregates, which are restricted by the stronger steric hindrance of the asphaltene matrix structure. This may make their chemical composition difficult to change during thermal evolution.

Table 3
Selected maturity parameters based on phenanthrene and methylphenanthrenes.

Fraction	R_o(%)	MPI_1	MPI_2	MPDF	MPR	MPR1	MPR2	MPR3	MPR9	∑MP/P
Free aromatics	0.55	0.30	0.34	0.51	1.62	0.09	0.14	0.11	0.15	0.49
	0.64	0.58	0.71	0.60	1.81	0.18	0.32	0.20	0.17	0.87
	0.92	1.24	1.68	0.55	1.54	1.12	1.72	0.81	0.96	4.61
	1.49	1.70	2.19	0.59	1.72	1.88	3.25	1.80	1.56	8.49
Adsorbed aromatics	0.55	0.16	0.18	0.53	1.82	0.04	0.06	0.05	0.07	0.22
	0.64	0.73	0.81	0.61	1.95	0.20	0.39	0.31	0.24	1.14
	0.92	0.77	0.93	0.59	1.82	0.27	0.48	0.31	0.29	1.35
	1.49	1.51	1.97	0.59	1.70	1.32	2.25	1.20	1.10	5.87
Occluded aromatics	0.55	1.31	1.60	0.60	1.90	0.67	1.27	0.81	0.71	3.46
	0.64	1.25	1.55	0.60	1.91	0.62	1.19	0.72	0.68	3.21
	0.92	1.27	1.60	0.60	1.86	0.67	1.24	0.74	0.67	3.32
	1.49	1.09	1.36	0.58	1.80	0.52	0.95	0.58	0.57	2.62

Notes: The R_o of the raw sample is approximately 0.55 % (Liang et al., 2020). The R_o of the samples after heat treatment is Easy%R_o (Sweeney and Burnham, 1990). MPI_1 = 1.5(2-MP + 3-MP)/(P + 1-MP + 9-MP), MPI_2 = 3(2-MP)/(P + 1-MP + 9-MP), (Radke, 1982); MPDF = (2-MP + 3-MP)/(1-MP + 9-MP + 2-MP + 3-MP), (Kvalheim et al., 1987); MPR = 2-MP/1-MP, (Radke, 1988); MPR1 = 1-MP/P, MPR2 = 2-MP/P, MPR3 = 3-MP/P, MPR9 = 9-MP/P, (Radke, 1982); ∑MP/P = (3-MP + 2-MP + 9-MP + 1-MP)/P. The full names of aromatic compounds are shown in Fig. 2.

Table 4
Selected maturity parameters based on chrysene and methylchrysenes.

Fraction	R_o(%)	MCI*	2-/1-MChy	1-/6-MChy	∑MChy/Chy
Free aromatics	0.55	1.01	0.92	1.42	1.41
	0.64	0.98	1.69	1.33	1.51
	0.92	1.53	1.59	1.93	3.10
	1.49	2.18	1.89	2.72	4.02
Adsorbed aromatics	0.55	0.72	1.75	1.36	0.84
	0.64	0.61	1.50	1.01	0.69
	0.92	0.69	1.61	1.77	0.91
	1.49	1.64	1.53	2.41	4.05
Occluded aromatics	0.55	0.62	1.88	0.93	0.65
	0.64	0.63	1.84	1.05	0.65
	0.92	0.39	1.90	1.31	0.36
	1.49	0.79	1.82	1.47	0.83

Notes: The R_o of the raw sample is approximately 0.55 % (Liang et al., 2020). The R_o of the samples after heat treatment is Easy%R_o (Sweeney and Burnham, 1990). MCI* = 1.5(2-MChy + 3-MChy)/(Chy + 1-MChy + 6-MChy) (compare "MCI_1'', (Garrigues et al., 1988)); ∑MChy/Chy = (3-MChy + 2-MChy + 6-MChy + 1-MChy)/Chy. The full names of aromatic compounds are shown in Fig. 3.

Table 5
Selected maturity parameters based on pyrene and methylpyrenes.

Fraction	R_o(%)	$MPyI_1$	$MPyI_2$	MPYR	2-/1-MPyr	∑MPyr/Pyr
Free aromatics	0.55	0.25	0.22	0.36	0.56	0.75
	0.64	0.38	0.24	0.39	0.64	1.41
	0.92	0.39	0.20	0.32	0.47	2.16
	1.49	0.75	0.37	0.47	0.88	2.93
Adsorbed aromatics	0.55	0.11	0.22	0.36	0.57	0.23
	0.64	0.46	0.50	0.58	1.36	0.66
	0.92	0.49	0.46	0.53	1.12	0.78
	1.49	0.70	0.35	0.45	0.82	2.81
Occluded aromatics	0.55	0.31	0.54	0.56	1.28	0.36
	0.64	0.23	0.50	0.54	1.20	0.27
	0.92	0.23	0.56	0.58	1.35	0.25
	1.49	0.33	0.53	0.56	1.27	0.41

Notes: The R_o of the raw sample is approximately 0.55 % (Liang et al., 2020). The R_o of the samples after heat treatment is Easy%R_o (Sweeney and Burnham, 1990). $MPyI_1$ = 3(2-MPyr)/(Pyr + 1-MPyr + 4-MPyr), $MPyI_2$ = (2-MPyr)/(1-MPyr + 4-MPyr) (Garrigues et al., 1988); MPYR = 2-MPyr/(1-MPyr + 2-MPyr) (Kruge, 2000); ∑MPyr/Pyr = (1-MPyr + 2-MPyr + 4-MPyr)/Pyr. The full names of aromatic compounds are shown in Fig. 4.

4.2 Differences in the thermal evolution of asphaltene-trapped methylated PAHs as compared to free PAHs

4.2.1 Evolution of adsorbed methylated PAHs

The relative proportions of the methylphenanthrene isomers showed similar evolution patterns in the free and adsorbed aromatics up to the reaction temperature of 350 °C (Fig. 9a). For the maturation temperature 400 °C, the relative proportion of free 1-MP decreased, while the relative proportion of 3-MP increased (Fig. 9a). The relative proportions of the free and adsorbed methylchrysenes also showed a parallel evolution up to a maturation temperature of 350 °C (Fig. 9b). For the 400 °C experiment, the relative proportion of free 1-MChy decreased, while the relative proportion of 3-MChy increased (Fig. 9b). The changes in the relative proportions of 1-MPyr and 2-MPyr were analogous to those of 1-MP and 3-MP (Fig. 9a & 9c).

In contrast to previous findings, the relative proportion of some β isomers in free and adsorbed methyl aromatic compounds (3-MP, 3-MChy, 2-MPyr) gradually decreased with thermal evolution below 350 °C, while the relative proportion of some α isomers (1-MP, 1-MChy, 1-MPyr) increased. The increase in the proportion of the less stable α-isomers implies that the distribution of free and adsorbed methylated aromatics is caused by their new formation rather than by the transformation of other less stable isomers.

The observed changes in the relative proportion of free methylated aromatics above 350 °C are consistent with the findings of previous studies (Radke, 1982; Kruge, 2000). Due to their higher stability, the consumption of the β isomers is slower than that of α isomers in the later stage of thermal evolution, resulting in a larger relative proportion of β isomers. In contrast, their relative proportion in the adsorbed methylated aromatics remained the same. We interpret this as the result of restriction/hindrance of the isomerization reaction due to a protection of the polyaromatic compounds by the asphaltene structure. This may lead difficulties in the demethylation of methylated aromatics in the late stage of thermal evolution.

4.2.2 Evolution of occluded methylated PAHs

The relative proportions of methylphenanthrene isomers in the occluded aromatics of all samples, including the original bitumen, did not vary significantly with temperature, with the abundances decreasing in the order 2-MP > 3-MP > 9-MP > 1-MP (Fig. 9a). The relative proportions of the methylchrysene isomers in the occluded aromatics of the original sample decrease in the order 3-MChy > 2-MChy > 6-MChy > 1-MChy, while the order of relative proportions in occluded methylchrysene isomers changed to 3-MChy > 2-MChy > 1-MChy > 6-MChy after thermal maturation (Fig. 9b). The ΔG values obtained from the quantum chemical calculations show that the order of thermal stability

Table 6
Calculated Gibbs free energies of methylated PAHs.

Methylated isomers		ΔG (kJ/mol) 25 °C,1 atm	ΔG (kJ/mol) 300 °C,296.08 atm	ΔG (kJ/mol) 350 °C,296.08 atm	ΔG (kJ/mol) 400 °C,296.08 atm
2-MP	β isomer	0.00	0.00	0.00	0.00
3-MP	β isomer	0.17	0.79	0.79	0.84
9-MP	α isomer	3.89	8.91	9.62	10.33
1-MP	α isomer	5.73	9.79	10.42	11.00
3-MChy	β isomer	0.00	0.00	0.00	0.00
2-MChy	β isomer	0.84	4.85	5.27	5.69
6-MChy	α isomer	1.34	10.17	10.92	47.86
1-MChy	α isomer	5.36	8.28	8.79	9.25
2-MPyr	β isomer	0.00	0.00	0.00	0.00
4-MPyr	α isomer	3.39	6.61	7.41	8.16
1-MPyr	α isomer	6.07	7.87	8.49	9.12

Notes: The full names of the isomers are shown in Figs. 2-4. ΔG was calculated by using the value for the isomer with the lowest Gibbs free energy as a reference.

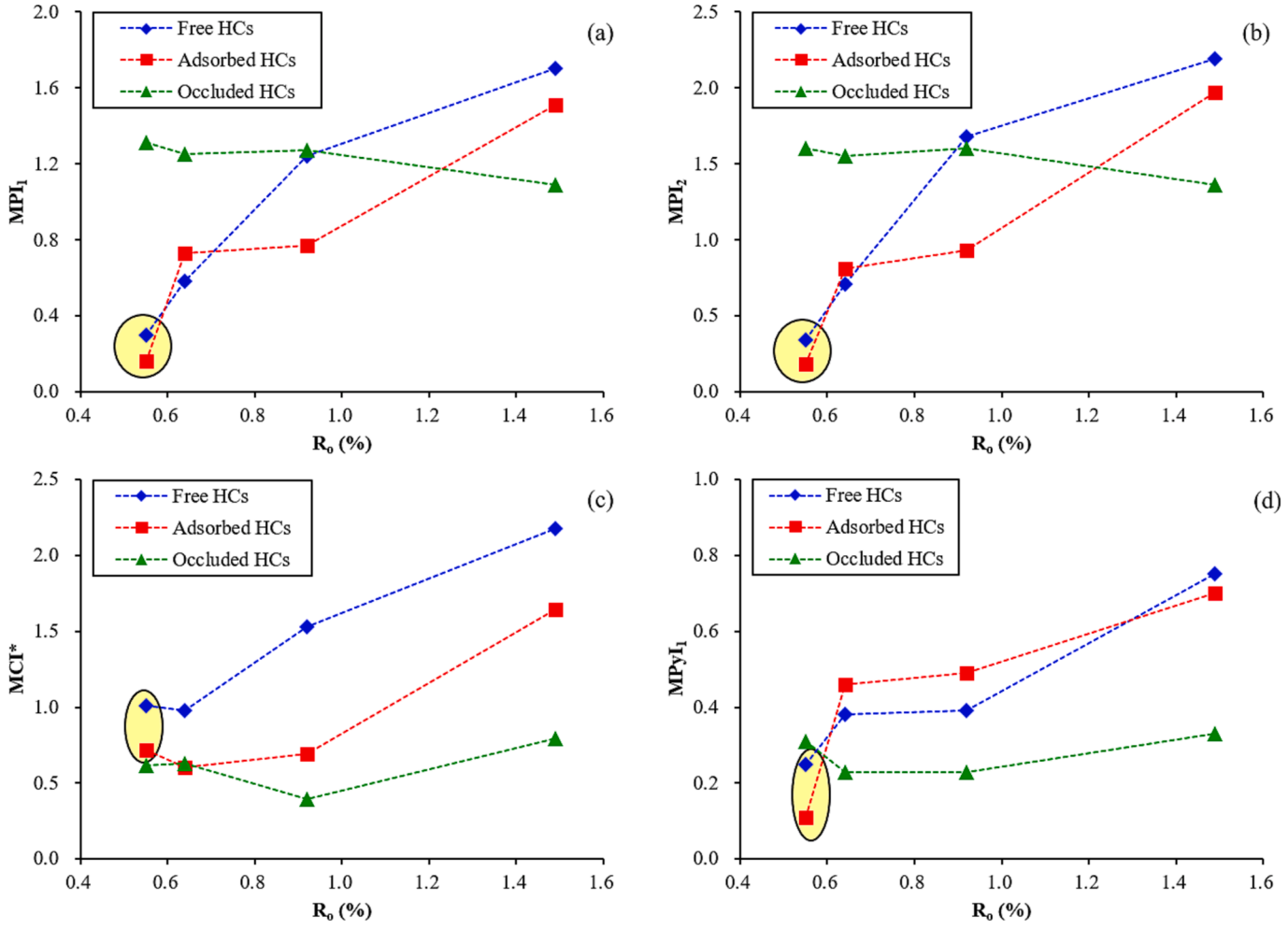

Fig. 5. Variations in some PAH-based parameters showing a correlation with R_o. The points in the yellow shaded fields correspond to the free and adsorbed aromatics of the original solid bitumen sample. (For interpretation of the references to colour in this figure legend, the reader is referred to the web version of this article.)

of the methylphenanthrene and methylchrysene isomers is consistent with the above experimental data, that is, isomers with higher stability show a higher relative content (Fig. 10a & b). It is thus inferred that the distributions of occluded methylphenanthrenes and methylchrysenes are mainly controlled by thermodynamics.

The quantum chemical calculations show that the ΔG value of 6-MChy increases with temperature, leading to a reversal of the thermal stability order of 1-MChy and 6-MChy (Fig. 10b). This significant decrease in the stability of the 6-MChy structure may lead to its higher susceptibility decomposition during heat treatment. Accordingly, in contrast to other isomer ratios for the occluded aromatics, 1-/6-MChy increased with temperature (Fig. 11). Similar changes in the 1-/6-MChy ratio in the free and adsorbed aromatics may also be related to the abrupt change in the thermal stability of 6-MChy (Fig. 11). We suggest that the 1-/6-MChy ratio in occluded aromatics is a potential maturity parameter.

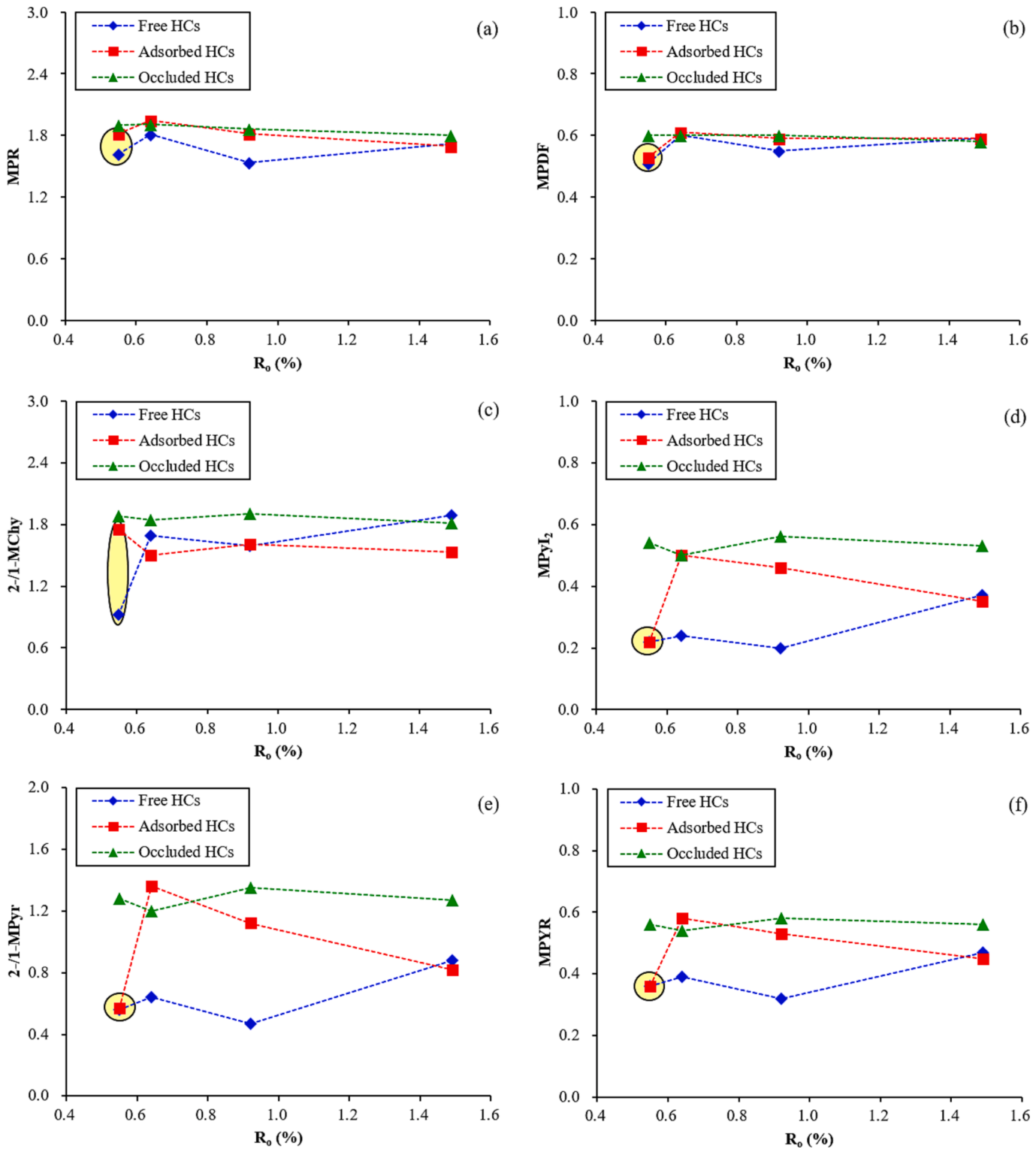

Fig. 6. Variations in some PAH-based parameters showing no correlation with R_o. The points in the yellow shaded fields correspond to the free and adsorbed aromatics of the original solid bitumen sample. (For interpretation of the references to colour in this figure legend, the reader is referred to the web version of this article.)

The computed ΔG values indicate that the thermal stability of the methylpyrene isomers decreases in the order 2-MPyr > 4-MPyr > 1-MPyr (Fig. 10c). However, the relative proportions of occluded methylpyrenes in this study were always found as 4-MPyr > 2-MPyr > 1-MPyr, indicating that the distribution of occluded methylpyrenes was not thermodynamically controlled (Fig. 9c). Pyrene homologs present in sedimentary rocks may come from some natural precursors or may break off and be released from kerogen macromolecules, resulting in a "source-controlled" distribution of methylpyrene compounds (Garrigues et al., 1988; Pehr et al., 2021). Additionally, methylpyrene is composed of relatively denser aromatic rings, leading to stronger intermolecular interactions with asphaltene structures, such as π-π stacking (Wu et al.,

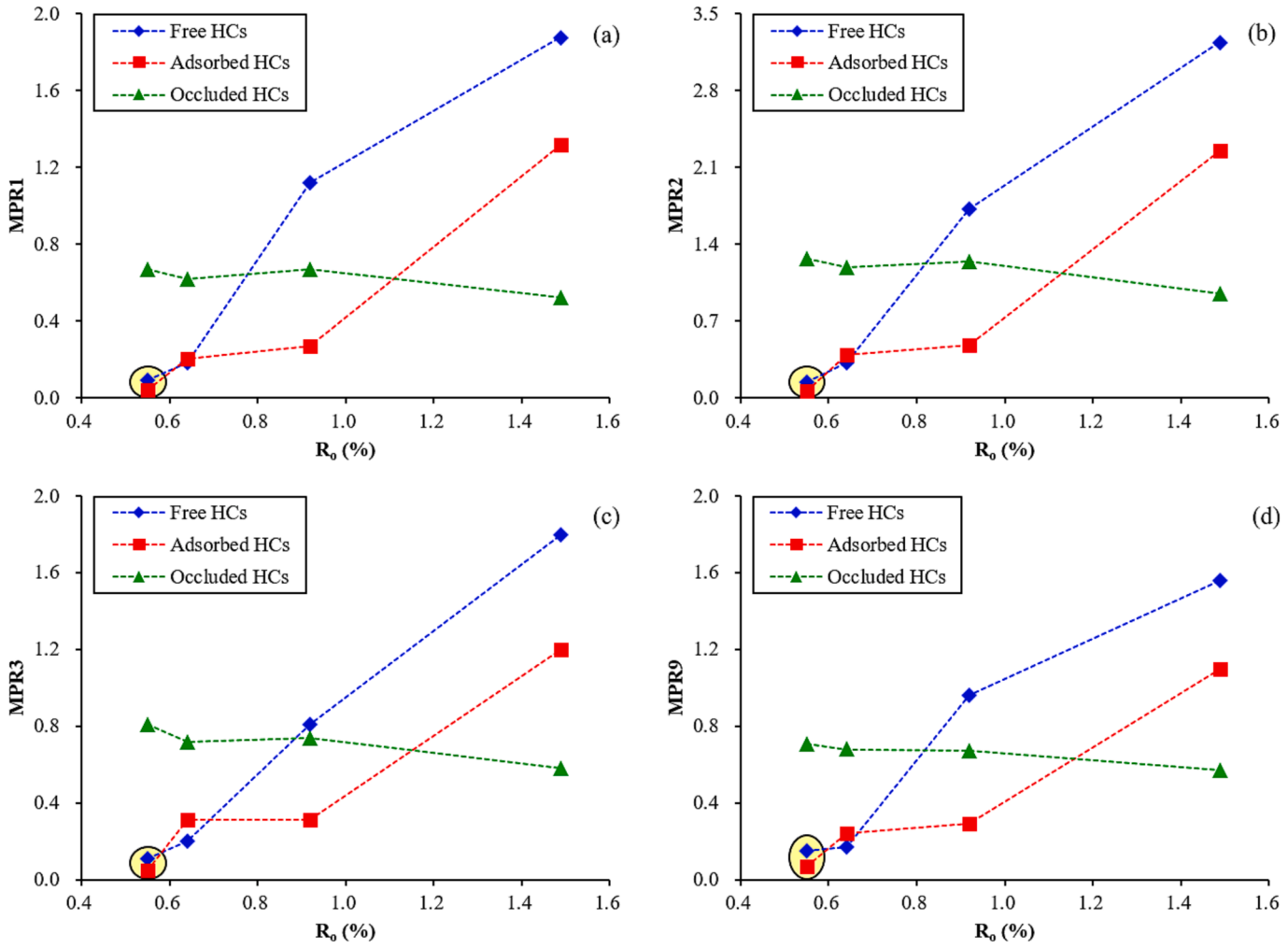

Fig. 7. Variations in MPR1, MPR2, MPR3, and MPR9 with R_o. The points in the yellow shaded fields correspond to the free and adsorbed aromatics of the original solid bitumen sample. (For interpretation of the references to colour in this figure legend, the reader is referred to the web version of this article.)

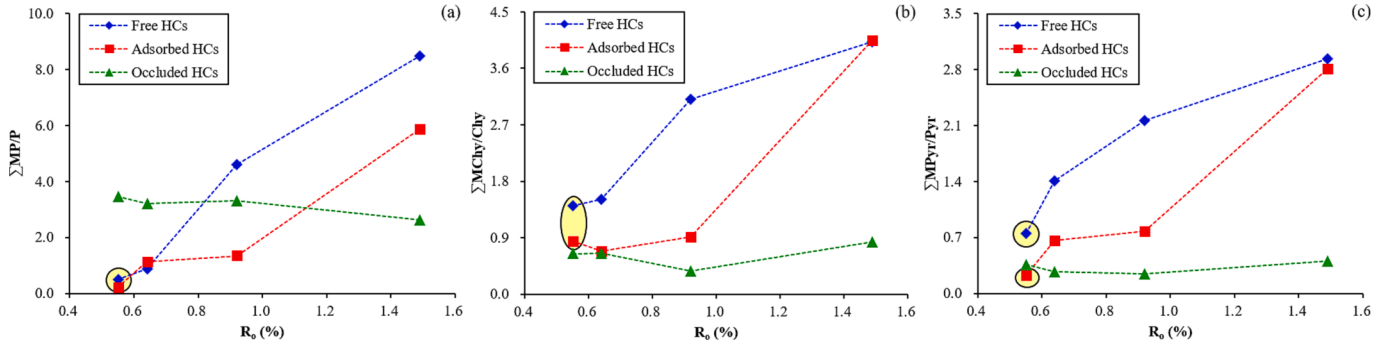

Fig. 8. Variations in ∑MP/P, ∑MChy/Chy, and ∑MPyr/Pyr with R_o. The points in the yellow shaded fields correspond to the free and adsorbed aromatics of the original solid bitumen sample. (For interpretation of the references to colour in this figure legend, the reader is referred to the web version of this article.)

2020). Thus, it is presumed that the methylpyrene isomers occluded in the asphaltene structure are more stable, less susceptible to thermal effects, and more likely to retain their original distribution.

4.3 Implications

4.3.1 "Protective effect" of the macromolecular asphaltene structure

According to present understanding, aromatic compounds trapped by the asphaltene matrix are confined to cavities formed by asphaltene nanoaggregates (Gray et al., 2011; Evdokimov, 2019; Scott et al., 2021). The macromolecular structure is assumed to produce a nanoconfinement effect, leading to significant changes in the physico-chemical behavior of trapped small molecules (Grommet et al., 2020; Yu et al., 2021). For instance, the asphaltene structure probably has a certain protective effect on small molecules, inhibiting the reactivity of small molecules while making it difficult for the groups that may initiate the reaction to form an effective attack path. Thus they act as a reaction inhibitor, reducing the reaction rate of small molecules (Miners et al.,

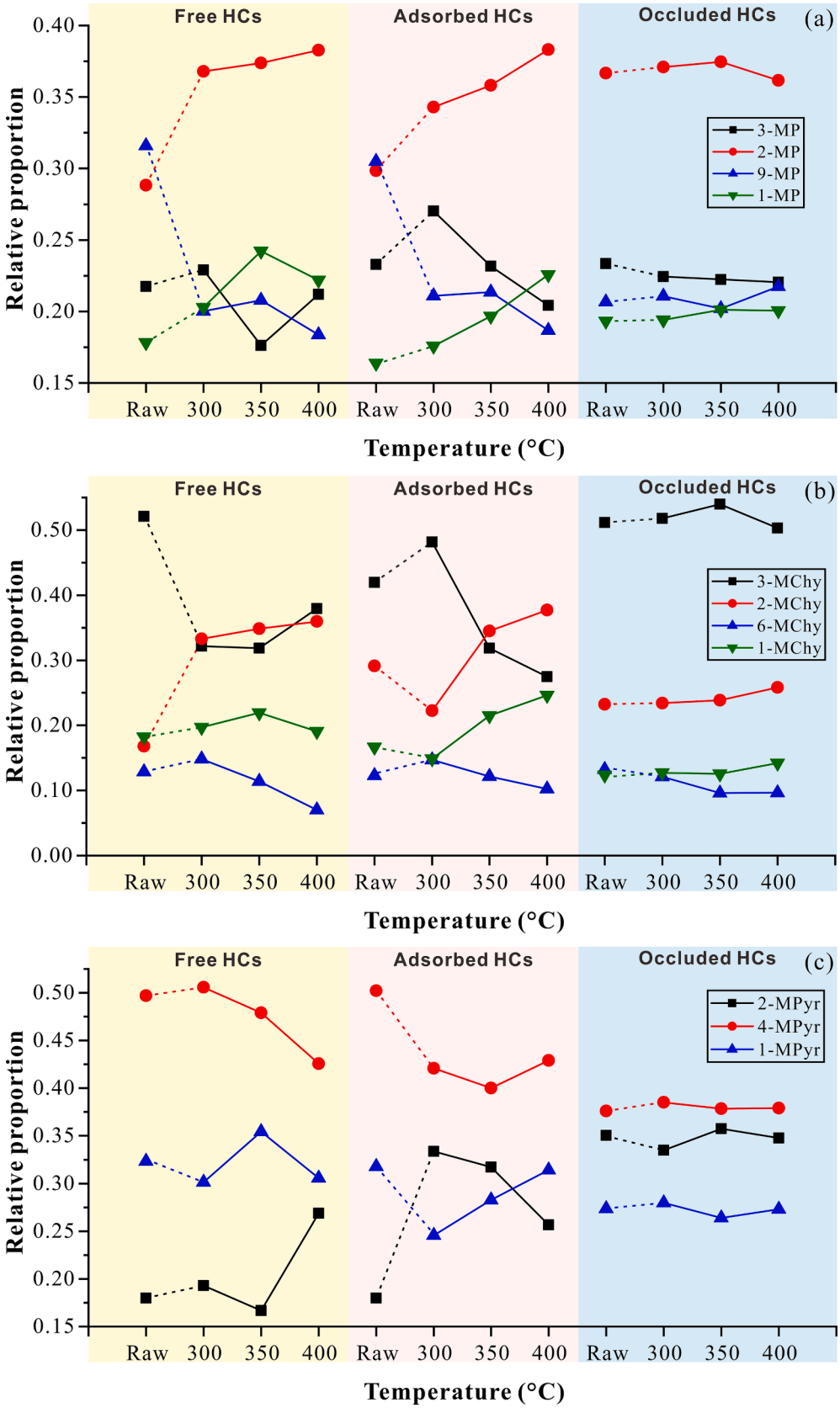

Fig. 9. Variation in relative proportions of methylated PAHs in the free, adsorbed and occluded aromatic fractions with temperature. (a) Methylphenanthrenes; (b) Methylchrysenes; (c) Methylpyrenes.

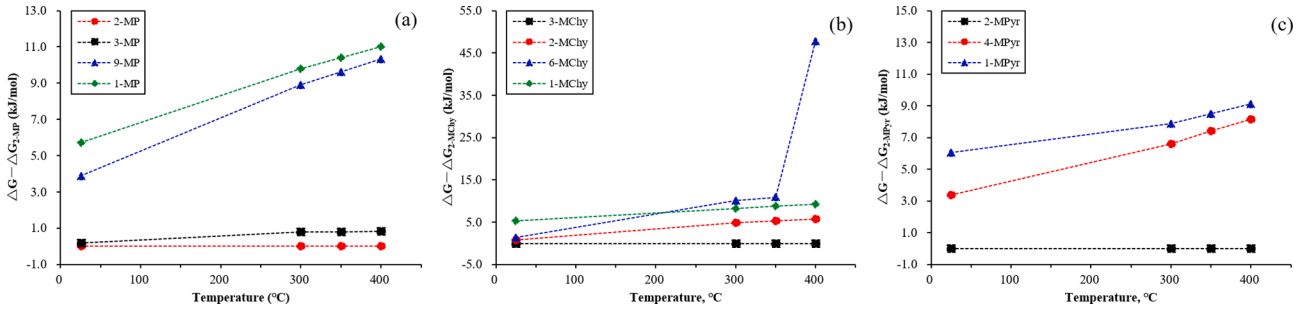

Fig. 10. ΔG of methylated PAHs under different temperature–pressure conditions (see Table 6). (a) Methylphenanthrenes; (b) Methylchrysenes; (c) Methylpyrenes.

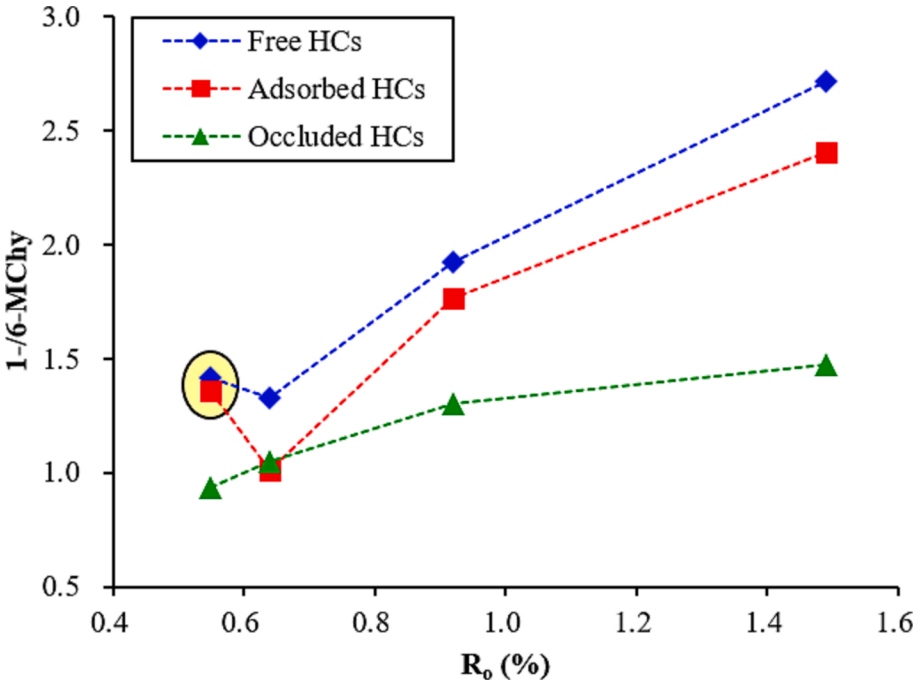

Fig. 11. Variation in 1-/6-MChy with R_o. The points in the yellow shaded field correspond to free and adsorbed aromatics of the original solid bitumen sample. (For interpretation of the references to colour in this figure legend, the reader is referred to the web version of this article.)

2016; Yang et al., 2019; Yu et al., 2021; Yang et al., 2022).

During the thermal evolution, the distributions of free and adsorbed aromatics are apparently controlled by reaction kinetics. The restriction of the asphaltene structure is thought to cause a large kinetic barrier, resulting in an obvious retardation in the thermal evolution of adsorbed aromatics. On the other hand, occluded aromatics exist in a relatively closed system composed of asphaltene nanoaggregates, and their distributions are mainly controlled by their thermal stability. Some PAHs (such as the methylpyrene isomers) appear to be particularly refractory because of their strong interaction with asphaltene structure in the occluded state.

4.3.2 Interpretation of PAH maturity parameters

Radke et al. (1984) proposed the empirical formula $R_c(\%) = 0.6MPI_1 + 0.4$ to calculate equivalent vitrinite reflectance values R_c from the methylphenanthrene index (MPI_1) (Fig. 12). The Easy%R_o model is an approach to relate the (measured) vitrinite reflectance value to the thermal (time–temperature) history of the kerogen (Sweeney and Burnham, 1990). Both models have been calibrated with different sample sets. Therefore, an exact correlation (1:1) of these parameters, although desirable, cannot be taken for granted. In the present study we have compared the vitrinite reflectance values derived for our samples with both models. A cross-plot of the Easy%R_o values and the R_c values calculated from the MPI_1 for the free, adsorbed and occluded aromatics of this study is shown in Fig. 12. The R_c values for the free and adsorbed aromatics show a reasonable to good approximation of the 1:1 slope (dR_c/dR_o = 0.74 and dR_c/dR_o = 0.86, respectively). Therefore, the empirical formulas of predecessors can be modified according to a large amount of geological sample data so that the MPI_1 of adsorbed aromatics can be used to estimate the maturity of organic matter.

At high thermal evolution stages, soluble asphaltene macromolecules in sedimentary organic matter are usually depleted, but there are still residual kerogen macromolecules. The small molecular aromatics restricted by the macromolecular structure of kerogen have similar evolution behavior as the aromatics trapped by asphaltene in theory (Brocks et al., 2003; Pehr et al., 2021). Therefore, the parameters calculated according to the aromatics adsorbed by macromolecules probably provide valuable results for the maturity assessment of high-maturity organic matter.

The R_c calculated from the MPI_1, of the occluded aromatics remain essentially constant around a value of 1.1 (Fig. 12). The slope of the linear regression bewteen R_c and R_o is −0.13 (approximately 0), indicating that R_c based on the occluded aromatics is not suitable for maturity assessment. However, due to their thermal stability, there may

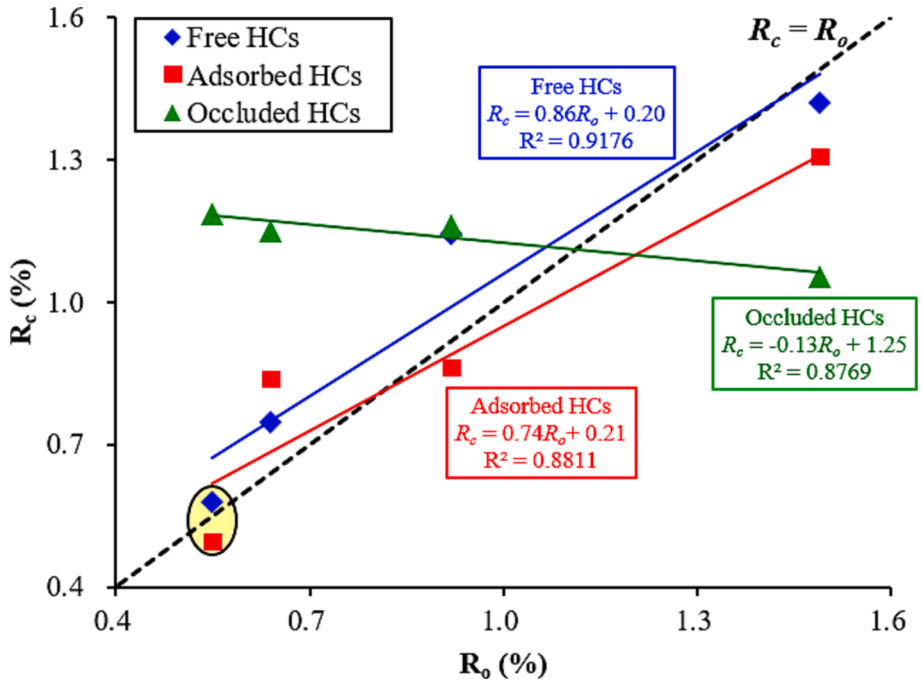

Fig. 12. Variation of R_c with R_o. The R_o of the original solid bitumen sample is approximately 0.55 % (Liang et al., 2020). R_o is the calculated vitrinite reflectance value of the samples after heat treatment based on the Easy%R_o model (Sweeney and Burnham, 1990). R_c is computed according to the formula R_c (%) = 0.6MPI_1 + 0.4 (Radke et al., 1984). The points in the yellow shaded field correspond to free and adsorbed aromatics of the original solid bitumen sample. (For interpretation of the references to colour in this figure legend, the reader is referred to the web version of this article.)

be some PAH-based parameters in occluded aromatics that can be used to assess the original composition of sedimentary organic matter (Yang et al., 2009; Tian et al., 2012a; Tian et al., 2012b).

5. Conclusions

(1) The increase in the aromatic maturity parameters (MPI, $MPyI_1$, MCI*) of the free and adsorbed components observed in the thermal maturation experiments on the Cambrian Changjianggou solid bitumen may be due to a continuous formation of methylated PAHs. The distributions of methylated PAHs in the free and adsorbed aromatics appear to be mainly kinetically controlled. We suspect that the asphaltene matrix acts as a reaction inhibitor for thermally induced isomerization reactions of the occluded/adsorbed aromatics, resulting in a retardation of the evolution of the aromatic maturity parameters. Due to this offset, the asphaltene-adsorbed aromatics may (if properly calibrated) provide a means to extend of the range of aromatic maturity parameters to organic matter with higher thermal maturity.

(2) The distributions of the occluded methylphenanthrene and methylchrysene isomers suggest that these compounds are in thermodynamic equilibrium. The asphaltene-occluded compounds have remained in a relatively closed system during long geologic periods of time, which is likely to have resulted in a thermodynamically controlled equilibrium distribution of some occluded PAHs. Other occluded PAHs (such as the methylpyrene isomers), due to high kinetic barriers (activation energies), are less likely to have reached thermodynamic equilibrium. Their isomer distribution, therefore, appears suitable as a source indicator for the sedimentary organic matter.

CRediT authorship contribution statement

Peng Fang: Methodology, Investigation, Formal analysis, Writing – original draft. **Zhibin Hong:** Writing – review & editing. **Jia Wu:** Methodology, Writing – review & editing, Funding acquisition. **Yuan Wang:** Data curation, Validation. **Keyu Liu:** Resources. **Minghui Zhou:** Writing – review & editing.

Declaration of Competing Interest

The authors declare that they have no known competing financial interests or personal relationships that could have appeared to influence the work reported in this paper.

Data availability

No data was used for the research described in the article.

Acknowledgments

The authors are grateful to Shuo Gao, Shengbao Shi and Lei Zhu for technical assistance of the experiments. Stephen R. Larter and Bernhard M. Krooss supplied helpful discussion. This study was funded by the State Key Laboratory of Petroleum Resources and Prospecting (No. PRP/indep-3-1715) and the State Key Laboratory of Organic Geochemistry (No. SKLOG202123). Computation time and software resources were provided by the High Performance Computing Center of Sichuan University of Science and Engineering in Zigong, China.

References

Brocks, J.J., Love, G.D., Snape, C.E., Logan, G.A., Summons, R.E., Buick, R., 2003. Release of bound aromatic hydrocarbons from late archean and mesoproterozoic kerogens via hydropyrolysis. Geochim. Cosmochim. Acta 67 (8), 1521–1530.

Castillo, J., Gonzalez, G., Bouyssiere, B., Vargas, V., 2023. Asphaltenes, Subfractions A1 and A2 Aggregation and Adsorption onto Rh-Sio2 nanoparticles: solvent effect on the aggregate size. Fuel 331, 125635.

Chacón-Patiño, M.L., Vesga-Martínez, S.J., Blanco-Tirado, C., Orrego-Ruiz, J.A., Gomez-Escudero, A., Combariza, M.Y., 2016. Exploring occluded compounds and their interactions with asphaltene networks using high-resolution mass spectrometry. Energy Fuel 30 (6), 4550–4561.

Chacón-Patiño, M.L., Rowland, S.M., Rodgers, R.P., 2017a. Advances in Asphaltene Petroleomics. Part 1: Asphaltenes Are Composed of Abundant Island and Archipelago Structural Motifs. Energy Fuel 31 (12), 13509–13518.

Chacón-Patiño, M.L., Rowland, S.M., Rodgers, R.P., 2017b. Advances in Asphaltene Petroleomics. Part 2: Selective Separation Method That Reveals Fractions Enriched in Island and Archipelago Structural Motifs by Mass Spectrometry. Energy Fuel 32 (1), 314–328.

Chacón-Patiño, M.L., Rowland, S.M., Rodgers, R.P., 2018. Advances in Asphaltene Petroleomics. Part 3. Dominance of Island or Archipelago Structural Motif Is Sample Dependent. Energy Fuel 32 (9), 9106–9120.
Chen, Z., Wen, Z., Zhang, C., He, Y., Gao, Y., Bai, X., Wang, X., 2023. A Study on the Applicability of Aromatic Parameters in the Maturity Evaluation of Lacustrine Source Rocks and Oils Based on Pyrolysis Simulation Experiments. ACS Omega 8 (30), 27674–27687.
Cheng, B., Du, J., Tian, Y., Liu, H., Liao, Z., 2016. Thermal Evolution of Adsorbed/Occluded Hydrocarbons inside Kerogens and Its Significance as Exemplified by One Low-Matured Kerogen from Santanghu Basin. Northwest China. Energy Fuels 30 (6), 4529–4536.
Cheng, B., Zhao, J., Yang, C., Tian, Y., Liao, Z., 2017. Geochemical Evolution of Occluded Hydrocarbons inside Geomacromolecules: A Review. Energy Fuel 31 (9), 8823–8832.
de Lima, A.L.B., da Silva, T.F., González, M.B., Peralba, M.d.C.R., Jural, P.A., Lenz, R.L., Barrionuevo, S., Dubois, D.S. and Spigolon, A.L.D., 2022. Characterization of Heavy Oils from the Campos Basin, Brazil: free biomarkers in oils, adsorbed and occluded in asphaltene structures. J. Petrol. Sci. Eng., 215: 110542.
Derakhshesh, M., Bergmann, A., Gray, M.R., 2013. Occlusion of Polyaromatic Compounds in Asphaltene Precipitates Suggests Porous Nanoaggregates. Energy Fuel 27 (4), 1748–1751.
Evdokimov, I.N., 2019. Colloidal Asphaltenes – Non-Extinct "Dinosaurs" in Native Petroleum. Energy Fuel 33 (9), 8440–8447.
Evdokimov, I.N., Losev, A.P., 2020. Asphaltene Solutions Are Not Adequately Described by Popular Models of Solid Suspensions. Energy Fuel 34 (7), 8007–8011.
Fang, R., Li, M., Wang, T.G., Zhang, L., Shi, S., 2015. Identification and Distribution of Pyrene, Methylpyrenes and Their Isomers in Rock Extracts and Crude Oils. Org Geochem. 83–84, 65–76.
Fang, P., Wu, J., Chen, F., Wang, Y., Wang, X.-C., Liu, K., Zhou, M., 2022a. The Hysteresis of Asphaltene-Trapped Saturated Hydrocarbons During Thermal Evolution. Fuel 329, 125374.
Fang, P., Wu, J., Li, B., Cheng, B., Song, D., Zhong, N., 2022b. Nondestructive Investigation on Hydrocarbons Occluded in Asphaltene Matrix: The Evidence from the Dispersive Solid-Phase Extraction. J. Pet. Sci. Eng. 217, 110890.
Garrigues, P., Sury, R.D., Angelin, M.L., Bellocq, J., Oudin, J.L., Ewald, M., 1988. Relation of the Methylated Aromatic Hydrocarbon Distribution Pattern to the Maturity of Organic Matter in Ancient Sediments from the Mahakam Delta. Geochim. Cosmochim. Acta 52 (2), 375–384.
González, G.n., Acevedo, S.c., Castillo, J., Villegas, O., Ranaudo, M.a.A., Guzmán, K., Orea, M., Bouyssiere, B., 2020. Study of very high molecular weight cluster presence in Thf Solution of Asphaltenes and Subfractions A1 and A2, by gel permeation chromatography with inductively coupled plasma mass spectrometry. Energy Fuels 34 (10), 12535–12544.
Gray, M.R., Tykwinski, R.R., Stryker, J.M., Tan, X., 2011. Supramolecular Assembly Model for Aggregation of Petroleum Asphaltenes. Energy Fuel 25 (7), 3125–3134.
Grommet, A.B., Feller, M., Klajn, R., 2020. Chemical Reactivity under Nanoconfinement. Nat. Nanotechnol. 15 (4), 256–271.
Huang, D., Li, J., Zhang, D., 1990. Maturation Sequence of Continental Crude Oils in Hydrocarbon Basins in China and Its Significance. Org Geochem. 16 (1), 521–529.
Kruge, M.A., 2000. Determination of Thermal Maturity and Organic Matter Type by Principal Components Analysis of the Distributions of Polycyclic Aromatic Compounds. Int. J. Coal Geol. 43 (1), 27–51.
Kvalheim, O.M., Christy, A.A., TelnæS, N., BjØRseth, A., 1987. Maturity Determination of Organic Matter in Coals Using the Methylphenanthrene Distribution. Geochim. Cosmochim. Acta 51 (7), 1883–1888.
Li, M., Shi, S., Wang, T.G., 2012. Identification and Distribution of Chrysene, Methylchrysenes and Their Isomers in Crude Oils and Rock Extracts. Org Geochem. 52, 55–66.
Li, M., Wang, H., Shi, S., Fang, R., Tang, Q., Wang, D., 2016. The Occurrence and Distribution of Phenylnaphthalenes, Terphenyls and Quaterphenyls in Selected Lacustrine Shales and Related Oils in China. Org Geochem. 95, 55–70.
Liang, T., Zhan, Z.W., Gao, Y., Wang, Y.P., Peng, P.A., 2020. Molecular Structure and Origin of Solid Bitumen from Northern Sichuan Basin. Mar. Pet. Geol. 122, 104654.
Liao, Z., Geng, A., Graciaa, A., Creux, P., Chrostowska, A., Zhang, Y., 2006a. Different Adsorption/Occlusion Properties of Asphaltenes Associated with Their Secondary Evolution Processes in Oil Reservoirs. Energy Fuel 20 (3), 1131–1136.
Liao, Z., Geng, A., Graciaa, A., Creux, P., Chrostowska, A., Zhang, Y., 2006b. Saturated Hydrocarbons Occluded inside Asphaltene Structures and Their Geochemical Significance, as Exemplified by Two Venezuelan Oils. Org Geochem. 37 (3), 291–303.
Liu, W., Liao, Y., Jiang, C., Pan, Y., Huang, Y., Wang, X., Wang, Y., Peng, P.A., 2022. Superimposed Secondary Alteration of Oil Reservoirs. Part Ii: The Characteristics of Biomarkers under the Superimposed Influences of Biodegradation and Thermal Alteration. Fuel 307, 121721.
Love, G.D., Snape, C.E., Carr, A.D., Houghton, R.C., 1996. Changes in Molecular Biomarker and Bulk Carbon Skeletal Parameters of Vitrinite Concentrates as a Function of Rank. Energy Fuel 10 (1), 149–157.
Lu, S., Zhao, X., Wang, Z., Liu, X., Huang, D., 1996. The Characteristics of Aromatic Products of Hydrocarbon Generated from Coal. Acta Pet. Sin. 17 (1), 47–53 in Chinese.
Miners, S.A., Rance, G.A., Khlobystov, A.N., 2016. Chemical Reactions Confined within Carbon Nanotubes. Chem. Soc. Rev. 45 (17), 4727–4746.
Mullins, O.C., 2010. The Modified Yen Model†. Energy Fuel 24 (4), 2179–2207.
Mullins, O.C., 2011. The Asphaltenes. Annu. Rev. Anal. Chem. 4, 393–418.
Mullins, O.C., Sabbah, H., Eyssautier, J., Pomerantz, A.E., Barré, L., Andrews, A.B., Ruiz-Morales, Y., Mostowfi, F., McFarlane, R., Goual, L., Lepkowicz, R., Cooper, T., Orbulescu, J., Leblanc, R.M., Edwards, J., Zare, R.N., 2012. Advances in Asphaltene Science and the Yen-Mullins Model. Energy Fuel 26 (7), 3986–4003.
Nomoto, S., Hagiwara, M., Nakano, Y., Shimoyama, A., 2001. A New Parameter for Maturity Determination of Organic Matter in Sediments Based on the Clay-Catalyzed Thermal Isomerization of Monomethylphenanthrenes. Bull. Chem. Soc. Jpn. 73 (6), 1437–1443.
Orea, M., López, L., Ranaudo, M.A., Faraco, A.K., 2021. Saturated Biomarkers Adsorbed and Occluded by the Asphaltenes of Some Venezuelan Crude Oils: Limitations in Geochemical Assessment and Interpretations. J. Pet. Sci. Eng. 206, 109048.
Pehr, K., Bisquera, R., Bishop, A.N., Ossa Ossa, F., Meredith, W., Bekker, A., Love, G.D., 2021. Preservation and Distributions of Covalently Bound Polyaromatic Hydrocarbons in Ancient Biogenic Kerogens and Insoluble Organic Macromolecules. Astrobiology 21 (9), 1049–1075.
Peters, K., Walters, C., Moldowan, J., 2004. The Biomarker Guide, 2nd ed. Cambridge University Press, Cambridge.
Radke, M., 1982. Geochemical Study on a Well in the Western Canada Basin: Relation of the Aromatic Distribution Pattern to Maturity of Organic Matter. Geochim. Cosmochim. Acta 46 (1), 1–10.
Radke, M., 1988. Application of Aromatic Compounds as Maturity Indicators in Source Rocks and Crude Oils. Mar. Pet. Geol. 5 (3), 224–236.
Radke, M., Leythaeuser, D., Teichmüller, M., 1984. Relationship between Rank and Composition of Aromatic Hydrocarbons for Coals of Different Origins. Org Geochem. 6, 423–430.
Radke, M., Welte, D.H., Willsch, H., 1986. Maturity Parameters Based on Aromatic Hydrocarbons: Influence of the Organic Matter Type. Org Geochem. 10 (1–3), 51–63.
Radke, M., Willsch, H., Teichmüller, M., 1990. Generation and Distribution of Aromatic Hydrocarbons in Coals of Low Rank. Org Geochem. 15 (6), 539–563.
Radke, M., Rullkötter, J., Vriend, S.P., 1994. Distribution of Naphthalenes in Crude Oils from the Java Sea: Source and Maturation Effects. Geochim. Cosmochim. Acta 58 (17), 3675–3689.
Robert, P., 1988. Organic Metamorphism and Geothermal History: Microscopic Study of Organic Matter and Thermal Evolution of Sedimentary Basins. Springer, Dordrecht.
Rospondek, M.J., Marynowski, L., Chachaj, A., Góra, M., 2009. Novel Aryl Polycyclic Aromatic Hydrocarbons: Phenylphenanthrene and Phenylanthracene Identification, Occurrence and Distribution in Sedimentary Rocks. Org Geochem. 40 (9), 986–1004.
Sadeghtabaghi, Z., Rabbani, A.R., Hemmati-Sarapardeh, A., 2021. Experimental Evaluation of Thermal Maturity of Crude Oil Samples by Asphaltene Fraction: Raman Spectroscopy and X-Ray Diffraction. J. Pet. Sci. Eng. 199, 108269.
Sadeghtabaghi, Z., Rabbani, A.R., Hemmati-Sarapardeh, A., 2022. New Indexes for Thermal Maturity Assessment Based on Asphaltene Fraction. J. Pet. Sci. Eng. 211, 110213.
Scott, D.E., Schulze, M., Stryker, J.M., Tykwinski, R.R., 2021. Deciphering Structure and Aggregation in Asphaltenes: Hypothesis-Driven Design and Development of Synthetic Model Compounds. Chem. Soc. Rev. 50 (16), 9202–9239.
Seifert, W.K., Moldowan, J.M., 1980. The Effect of Thermal Stress on Source-Rock Quality as Measured by Hopane Stereochemistry. Phys. Chem. Earth 12, 229–237.
Snowdon, L.R., Volkman, J.K., Zhang, Z., Tao, G., Liu, P., 2016. The Organic Geochemistry of Asphaltenes and Occluded Biomarkers. Org Geochem. 91, 3–15.
Spiro, B., 1984. Effects of the Mineral Matrix on the Distribution of Geochemical Markers in Thermally Affected Sedimentary Sequences. Org Geochem. 6, 543–559.
Sweeney, J., Burnham, A., 1990. Evaluation of a Simple Model of Vitrinite Reflectance Based on Chemical Kinetics. AAPG Bull. 74 (10), 1559–1570.
Tannenbaum, E., Ruth, E., Kaplan, I.R., 1986. Steranes and Triterpanes Generated from Kerogen Pyrolysis in the Absence and Presence of Minerals. Geochim. Cosmochim. Acta 50 (5), 805–812.
Tian, Y., Yang, C., Liao, Z., Zhang, H., 2012a. Geochemical Quantification of Mixed Marine Oils from Tazhong Area of Tarim Basin, Nw China. J. Pet. Sci. Eng. 90–91, 96–106.
Tian, Y., Zhao, J., Yang, C., Liao, Z., Zhang, L., Zhang, H., 2012b. Multiple-Sourced Features of Marine Oils in the Tarim Basin, Nw China – Geochemical Evidence from Occluded Hydrocarbons inside Asphaltenes. J. Asian Earth Sci. 54–55, 174–181.
Tissot, B.P., Pelet, R., Ungerer, P.H., 1987. Thermal History of Sedimentary Basins, Maturation Indices, and Kinetics of Oil and Gas Generation1. AAPG Bull. 71 (12), 1445–1466.
Tissot, B.P., Welte, D.H., 1984. Petroleum Formation and Occurrence. Springer, Berlin, Heidelberg, New York.
Wang, X., Li, M., Yang, T., Zeng, B., Shi, Y., Liu, X., Tang, Y., 2023. Identification, Distribution and Geochemical Significance of Benzo[B]Naphthofurans and Benzo[B]Naphthothiophenes in Source Rocks from the Beibuwan Basin, South China Sea. Chem. Geol. 626, 121454.
Weigend, F., Ahlrichs, R., 2005. Balanced Basis Sets of Split Valence, Triple Zeta Valence and Quadruple Zeta Valence Quality for H to Rn: Design and Assessment of Accuracy. PCCP 7 (18), 3297–3305.
Wu, J., Qi, W., Luo, Q., Chen, Q., Shi, S., Li, M., Zhong, N., 2019. Experiments on the Generation of Dimethyldibenzothiophene and Its Geochemical Implications. Pet. Geol. Exp. 41 (2), 260–267 in Chinese.
Wu, J., Fang, P., Wang, X.-C., Li, B., Liu, K., Ma, X., Li, S., Li, M., 2020. The Potential Occurrence Modes of Hydrocarbons in Asphaltene Matrix and Its Geochemical Implications. Fuel 278, 118233.
Yang, Y., Hu, X., Zhang, C., Chen, Y., Zhen, J., Qin, L., 2022. Theoretical Study of the Formation of Large, Astronomically Relevant Pah-Organic Molecule Clusters. A & A 663, A52.
Yang, S., Li, M., Liu, X., Han, Q., Wu, J., Zhong, N., 2019. Thermodynamic Stability of Methyldibenzothiophenes in Sedimentary Rock Extracts: Based on Molecular Simulation and Geochemical Data. Org Geochem. 129, 24–41.

Yang, C., Liao, Z., Zhang, L., Creux, P., 2009. Some Biogenic-Related Compounds Occluded inside Asphaltene Aggregates. Energy Fuel 23 (1), 820–827.
Yu, Z., Lu, X., Sun, L., Xiong, J., Ye, L., Li, X., Zhang, R., Ji, N., 2021. Metal-Loaded Hollow Carbon Nanostructures as Nanoreactors: Microenvironment Effects and Prospects for Biomass Hydrogenation Applications. ACS Sustain. Chem. Eng. 9 (8), 2990–3010.
Zhao, J., Liao, Z., Zhang, L., Creux, P., Yang, C., Chrostowska, A., Zhang, H., Graciaa, A., 2010. Comparative Studies on Compounds Occluded inside Asphaltenes Hierarchically Released by Increasing Amounts of H2o2/Ch3cooh. Appl. Geochem. 25 (9), 1330–1338.
Zhao, J., Liao, Z., Chrostowska, A., Liu, Q., Zhang, L., Graciaa, A., Creux, P., 2012. Experimental studies on the adsorption/occlusion phenomena inside the macromolecular structures of asphaltenes. Energy Fuel 26 (3), 1746–1755.
Zhao, Y., Truhlar, D.G., 2008. Density functionals with broad applicability in chemistry. Acc. Chem. Res. 41 (2), 157–167.
Zhu, Z., Li, M., Tang, Y., Qi, L., Leng, J., Liu, X., Xiao, H., 2019. Identification of phenyldibenzothiophenes in coals and the effects of thermal maturity on their distributions based on geochemical data and theoretical calculations. Org Geochem. 138, 103910.
Zhu, Z., Li, M., Li, J., Qi, L., Liu, X., Xiao, H., Leng, J., 2022. Identification, distribution and geochemical significance of dinaphthofurans in coals. Org. Geochem. 166, 104399.